8-19-2005

Magnetic Inversion Symmetry Breaking and Ferroelectricity in $TbMnO_3$

Michel Kenzelmann

A. Brooks Harris
University of Pennsylvania, harris@sas.upenn.edu

Seth H. Jonas

Collin L. Broholm

Jürg Schefer

See next page for additional authors

Recommended Citation

Kenzelmann, M., Harris, A., Jonas, S. H., Broholm, C. L., Schefer, J., Kim, S., Zhang, C., Cheong, S., Vajk, O. P., & Lynn, J. W. (2005). Magnetic Inversion Symmetry Breaking and Ferroelectricity in $TbMnO_3$. *Physical Review Letters, 95* 087206-1-087206-4. http://dx.doi.org/10.1103/PhysRevLett.95.087206

Magnetic Inversion Symmetry Breaking and Ferroelectricity in $TbMnO_3$

Abstract

$TbMnO_3$ is an orthorhombic insulator where incommensurate spin order for temperature T_N<41 K is accompanied by ferroelectric order for>T<28 K. To understand>this, we establish the magnetic structure above and below the ferroelectric transition using neutron diffraction. In the paraelectric phase, the spin structure is incommensurate and longitudinally modulated. In the ferroelectric phase, however, there is a transverse incommensurate spiral. We show that the spiral breaks spatial inversion symmetry and can account for magnetoelectricity in $TbMnO_3$.

Disciplines

Physics

Author(s)

Michel Kenzelmann, A. Brooks Harris, Seth H. Jonas, Collin L. Broholm, Jürg Schefer, Sungbaek Kim, Chunli Zhang, Sangwook Cheong, Owen P. Vajk, and Jeffrey W. Lynn

Magnetic Inversion Symmetry Breaking and Ferroelectricity in $TbMnO_3$

M. Kenzelmann,[1,2,3] A. B. Harris,[4] S. Jonas,[3] C. Broholm,[3,5] J. Schefer,[2] S. B. Kim,[6] C. L. Zhang,[6] S.-W. Cheong,[6] O. P. Vajk,[5] and J. W. Lynn[5]

[1]*Laboratory for Solid State Physics, ETH Hönggerberg, CH-8093 Zürich, Switzerland*
[2]*Laboratory for Neutron Scattering, ETH Zürich and Paul Scherrer Institute, CH-5232 Villigen, Switzerland*
[3]*Department of Physics and Astronomy, Johns Hopkins University, Baltimore, Maryland 21218, USA*
[4]*Department of Physics and Astronomy, University of Pennsylvania, Philadelphia, Pennsylvania 19104, USA*
[5]*NIST Center for Neutron Research, National Institute of Standards and Technology, Gaithersburg, Maryland 20899, USA*
[6]*Department of Physics & Astronomy, Rutgers University, 136 Frelinghuysen Rd., Piscataway, New Jersey 08854, USA*

(Received 12 April 2005; published 19 August 2005)

$TbMnO_3$ is an orthorhombic insulator where incommensurate spin order for temperature $T_N < 41$ K is accompanied by ferroelectric order for $T < 28$ K. To understand this, we establish the magnetic structure above and below the ferroelectric transition using neutron diffraction. In the paraelectric phase, the spin structure is incommensurate and longitudinally modulated. In the ferroelectric phase, however, there is a transverse incommensurate spiral. We show that the spiral breaks spatial inversion symmetry and can account for magnetoelectricity in $TbMnO_3$.

DOI: 10.1103/PhysRevLett.95.087206 PACS numbers: 77.80.Bh, 75.10.Jm, 75.25.+z, 75.40.Gb

The coexistence of antiferromagnetism and ferroelectricity in solid materials is rare, and much rarer still is a strong coupling between these two order parameters [1,2]. In nonmagnetic perovskites like $BaTiO_3$, ferroelectricity is driven by a hybridization of empty d orbitals with occupied p orbitals of the octahedrally coordinated oxygen ions [3]. This mechanism requires empty d orbitals and thus cannot lead to magnetic ferroelectric materials. In materials such as $BiMnO_3$, lone s^2 electron pairs can lower their energy by hybridizing with empty p orbitals [4]. While it leads to coexistence of magnetic order with electric polarization at low temperatures, the very different ordering temperatures show that the two order parameters lower the symmetry of the systems through distinctly different collective effects.

$TbMnO_3$ is an antiferromagnet which contains Mn^{3+} ions with occupied d orbitals and no lone s^2 cation [5]. So, as for a number of recently discovered multiferroics [6–8], neither of the mechanisms described above can explain the coexistence of magnetic and electric order. In these materials, a magnetic field of a few Tesla can switch the direction of the electric polarization [5]—proof of a strong direct coupling between the magnetic and electric polarization. Rare-earth manganese oxides show a plethora of exciting phenomena which arise from competing interactions. $LaMnO_3$ is the parent compound to a series of materials featuring colossal magnetoresistance, and shows orbital ordering of its e_g orbital, giving rise to layered antiferromagnetic ordering. With decreasing rare-earth size, there is a tendency towards incommensurate magnetic order. Ferroelectric ground states were recently predicted for doped manganites of the type $R_{1-x}Ca_xMnO_3$, but they have not yet been observed [9]. The coexistence and strong coupling of ferroelectricity and antiferromagnetism in $TbMnO_3$ suggests the presence of a nonconventional coupling mechanism involving competing spin interactions, and it is thus of both practical and fundamental importance.

To develop a microscopic theory of the new coupling mechanism, unambiguous determination of the symmetry of the magnetic order is essential. In this Letter, we present neutron diffraction measurements of orthorhombic $TbMnO_3$, which determine the magnetic ground states and the phase diagram as a function of temperature and a magnetic field $\mathbf{H} \parallel \mathbf{a}$. We find that the ferroelectric phase transition coincides with a magnetic transition from a longitudinal incommensurate structure to an incommensurate spiral structure that breaks spatial inversion symmetry. We show that a recent theory proposed for axial-nonaxial parity breaking [10,11] predicts the observed orientation of the ferroelectric polarization based on the symmetry of the magnetic structure that we report.

$TbMnO_3$ crystals were grown using an optical floating zone furnace. A measurement of the temperature dependence of the dielectric constant of the two samples which we studied confirmed ferroelectricity below $T = 26$ K and $T = 28$ K for samples 1 and 2, respectively. The discrepancy may result from slightly differing oxygen partial pressure during annealing. The space group is No. 62, and in the Pbnm setting the lattice parameters are $a = 5.3$ Å, $b = 5.86$ Å, and $c = 7.49$ Å. The measurements were performed on two single-crystals weighing 40 and 220 mg, respectively, with the BT2 and SPINS spectrometers at NIST, and the TriCS 4-circle diffractometer at PSI.

The wave-vector dependence of the diffraction intensity along the $(0, k, 1)$ direction of reciprocal space (Figs. 1 and 2) illustrates the temperature dependence of magnetic order in $TbMnO_3$. Mn^{3+} spins develop long-range order at $T_N = 41$ K [12,13]. Immediately below the transition temperature, magnetic Bragg peaks are observed at $(0, 1 - q, 1)$ and $(0, q, 1)$ positions. At 35 K the magnetic order is described by a single Fourier component associated with a wave vector $(0, q, 0)$ with $q = 0.27$, and no apparent higher-order Fourier components. Upon cooling below

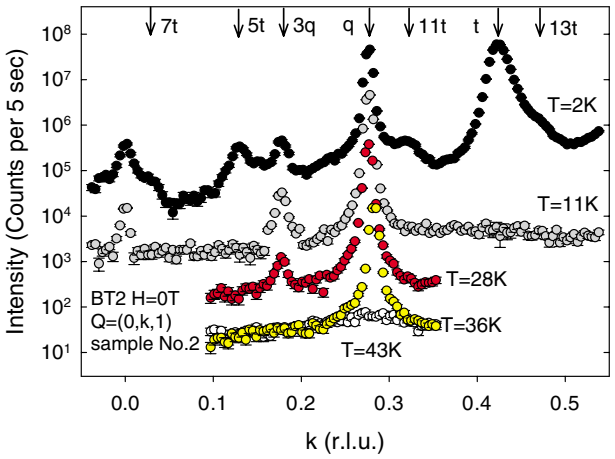

FIG. 1 (color online). Diffraction intensity along the $(0, k, 1)$ direction for different temperatures (with a factor 10 offset between the sub-T_N data sets), showing fundamental and higher-order Fourier components of the magnetic ordering. The $3t$- and $9t$-order peaks associated with the Tb order occur at $k = 0.725$ and 0.175, respectively, and are difficult to identify unambiguously due to their proximity to strong peaks.

$T = 28$ K, third-order magnetic Bragg peaks $(0, 1 - 3q, 0)$ appear (Fig. 1), indicating steplike modulation of the magnetic moment. The inset to Fig. 2(b) shows that the wave vector continues to vary with temperature throughout the ferroelectric phase.

Below $T = 7$ K, additional magnetic peaks appear that are associated with Tb moments and indicate that their interactions favor a different ordering wave vector than for the Mn moments. At $T = 2$ K, there is a strong peak at $(0, t, 1)$ with $t = 0.425$, and several higher-order peaks as indicated in Fig. 1. The many strong odd high-order reflections indicate that the order associated with the $(0, t, 0)$ wave vector is strongly distorted (bunched structure) as expected for anisotropic rare-earth magnets. The correlation length and the incommensuration of the Tb order at low temperatures is sample dependent, as is often found in systems with phase transitions between incommensurate structures. The correlation length along the b axis was 58(20) and 280(20) Å, and t was 0.41 and 0.425 in samples 1 and 2, respectively.

The magnetic structures at $T = 15$ and 35 K were determined from up to 922 first-order magnetic Bragg peaks each. Only first-order peaks were included in the refinement as these are sufficient to determine the symmetry of the magnetic structure. Representational analysis was used to find the irreducible representations that describe the magnetic structures. The structure at $T = 35$ K in the high-temperature incommensurate (HTI) phase can be described by a single irreducible representation. The best fit with $\chi^2 = 0.86$ was obtained for a structure described by representation Γ_3, and the excellent agreement between the model and the data is shown in Fig. 3(a). The magnetic structure is described by $\mathbf{m}_3^{\mathrm{Mn}} = [0.0(8), 2.90(5), 0.0(5)]\mu_B$ and $\mathbf{m}_3^{\mathrm{Tb}} = [0, 0, 0.0(4)]\mu_B$ where the subscript denotes the irreducible representation indicated in Fig. 4(c). The magnetic structure is longitudinally modulated with moment along the b axis, as illus-

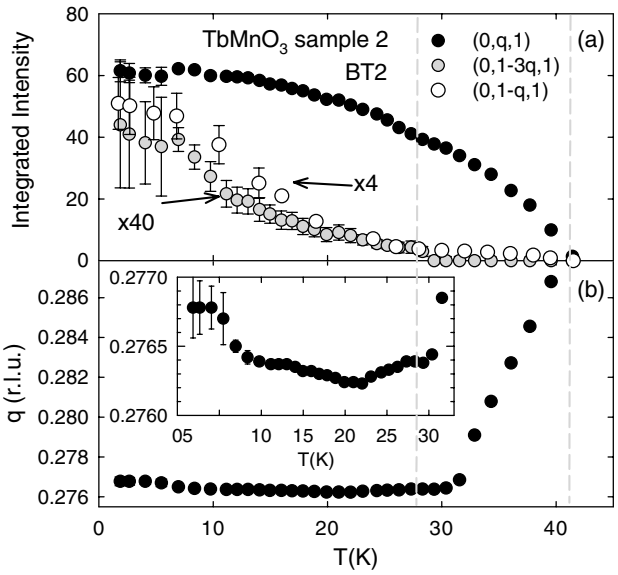

FIG. 2. (a) T dependence of the integrated intensity of the $(0, q, 1)$ Bragg peak and the associated third-order peak at $(0, 1 - 3q, 1)$. (b) T dependence of the wave vector q, corrected for the T dependence of the b lattice parameter, showing the absence of a lock-in transition at $T = 28$ K.

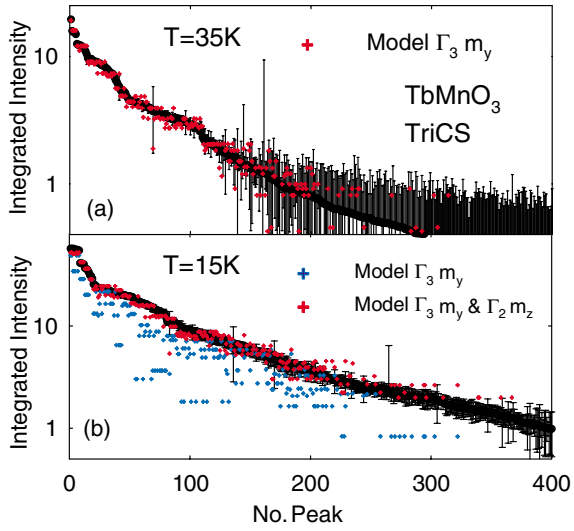

FIG. 3 (color). Integrated intensities of magnetic Bragg peaks measured at $T = 15$ K and $T = 35$ K using TriCS are compared to various magnetic structures. Peaks are sorted by decreasing measured intensity. (a) The $T = 35$ K structure is described by a single irreducible representation, Γ_3, and the moments point along the b axis. (b) The $T = 15$ K magnetic structure is a spiral described by a y component of Γ_3 and an x component of Γ_2 with a $\pi/2$ phase shift.

trated in Fig. 4(a) and consistent with an earlier study [12]. The absence of observable higher-order peaks indicates that the magnetic structure at $T = 35$ K is sinusoidally modulated.

Two irreducible representations are required to describe the magnetic structure at $T = 15$ K in the low-temperature incommensurate (LTI) phase. We found best agreement with $\chi^2 = 2.19$ for magnetic ordering involving Γ_2 and Γ_3, as shown in Fig. 3(b). Fits using the Γ_1 and Γ_3, or the Γ_3 and Γ_4 representation pairs led to $\chi^2 = 14.5$ and higher, and can thus be excluded. Neglecting higher-order reflections, the magnetic structure is given by $\mathbf{m}_3^{\mathrm{Mn}} = (0.0(5), 3.9(1), 0.0(7))\mu_B$, $\mathbf{m}_3^{\mathrm{Tb}} = (0, 0, 0(1))\mu_B$, $\mathbf{m}_2^{\mathrm{Mn}} = (0.0(1), 0.0(8), 2.8(1))\mu_B$, and $\mathbf{m}_2^{\mathrm{Tb}} = (1.2(1), 0(1), 0)\mu_B$. The experiment was not sensitive to the phase between the y and z component of the Mn moment. From the size of the moment, however, we deduce that the Mn moments form an elliptical spiral. The data did not favor a phase difference between the Tb and Mn moments, so these phases remain undetermined. Symmetry splits the Tb moments into two orbits which representation theory normally treats as independent. However, as suggested by Landau theory [10], we took these two Tb amplitudes to be identical. The phase between the two orbits was found to be to $1.3(3)\pi$. The greatly improved fit is evidence that the Tb sublattice carries significant magnetization in the LTI phase, presumably as a consequence of the exchange field from the ordered Mn sublattice.

Figs. 5(a) and 5(b) show the field dependence of the $(0, q, 1)$ magnetic Bragg reflection, which arises from the Mn spin spiral. Both the position and the intensity are field independent to within errorbar—evidence that the structure remains a spiral up to at least 6 T. Our calculations show that the intensity should drop by 7% if the z component of Γ_2 were extinguished. In contrast, no decrease is observed to within an error bar of 2% between 0 and 6 T.

The $(0, 1 - q, 1)$ Bragg reflection shown in Fig. 5(a) arises from Mn Γ_3 magnetization along the a axis and from Tb Γ_2 magnetization along the a axis. Because the x component of the Mn moment is small, the $(0, 1 - q, 1)$ Bragg reflection is particularly sensitive to Tb order. For $T < 28$ K the $(0, 1 - q, 1)$ intensity is suppressed by a field $\mathbf{H} \parallel \mathbf{a}$ confirming that the modulated Tb moment is oriented along that direction. Below the Tb ordering temperature, the field dependent magnetic Bragg intensity has a finite-field maximum [Fig. 5(a)], indicating a spin-flop transition.

We collected 51 magnetic Bragg peaks at $T = 4$ K and $H = 4$ T along $\mathbf{a}$ to determine the magnetic structure at low temperatures above the critical field for $(0, t, 0)$ Tb order [Fig. 5(c)]. The magnetic structure can be described by Γ_2 and Γ_3 with $\chi^2 = 3.81$ or by Γ_1 and Γ_3 with $\chi^2 = 4.19$. Since a field along the a direction disfavors antiparallel spin alignment in the same direction as in the Γ_1-Γ_3 structure, we infer that the structure is given by $\mathbf{m}_3^{\mathrm{Mn}} = [0.3(4), 4.7(3), 0.0(5)]\mu_B$, $\mathbf{m}_3^{\mathrm{Tb}} = [0, 0, 0.0(3)]\mu_B$, $\mathbf{m}_2^{\mathrm{Mn}} = [0.0(2), 0.0(4), 3.0(3)]\mu_B$, and $\mathbf{m}_2^{\mathrm{Tb}} = [0.3(2), 0.0(4), 0]\mu_B$. This result suggests that the spin spiral struc-

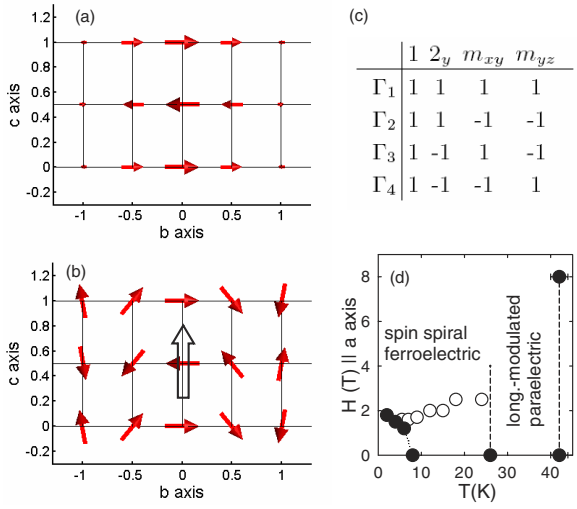

	1	2_y	m_{xy}	m_{yz}
Γ_1	1	1	1	1
Γ_2	1	1	-1	-1
Γ_3	1	-1	1	-1
Γ_4	1	-1	-1	1

FIG. 4 (color online). Schematic of the magnetic structure at (a) $T = 35$ K and (b) $T = 15$ K, projected onto the b-c plane. Filled arrows indicate direction and magnitude of Mn moments. The longitudinally modulated phase (a) respects inversion symmetry along the c axis, but the spiral phase (b) violates it, allowing an electric polarization (unfilled arrow). (c) Irreducible representation of the group $G_{\mathbf{k}}$ for the incommensurate magnetic structure with $\mathbf{k} = (0, q, 0)$. (d) Phase diagram as a function of temperature and field applied along the a axis. Solid circles indicate second order phase transitions. Open circles indicate the characteristic field for reduction of magnetic $(0, 1 - q, 1)$ Bragg scattering from Tb moments by 50% from its zero-field intensity.

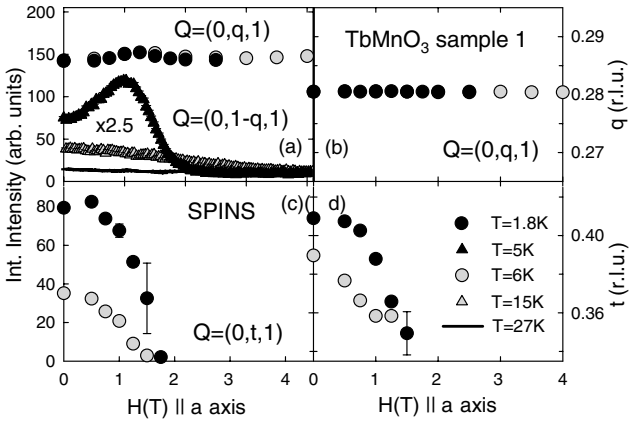

FIG. 5. Field dependence of magnetic Bragg scattering from $TbMnO_3$. (a) and (b) show data for the incommensurate peaks that occur for $T < 41$ K. (a) The $(0, q, 1)$ peak that is mostly sensitive to staggered magnetization on Mn sites and the $(0, 1 - q, 1)$ peak that is sensitive to staggered magnetization on Tb sites. (c) and (d) show data for the incommensurate peaks that develop for $T < 7$ K.

ture is more stable for fields along the a axis than for fields along the b axis [5].

Harris *et al.* [10,11] recently showed that insulators with axial-nonaxial parity breaking magnetic phase transitions must also be electrically polarized. Given the magnetic structure and the temperature dependence of the magnetic order parameter, the theory predicts the direction and temperature dependence of the electric polarization resulting from a symmetry allowed trilinear coupling term. In the following we show that this theory correctly accounts for the direction of the electric polarization in the LTI phase of $TbMnO_3$, and the absence of electric polarization in the HTI phase. The trilinear magnetoelectric coupling term in the Landau free energy expansion is written as $V = \Sigma_{uv\gamma} a_{uv\gamma} \sigma_u(k) \sigma_v(-k) P_\gamma$. Here $\sigma_u(k)$ is the magnetic order parameter of irreducible representation Γ_u, P_γ is the electric polarization along the γ crystallographic direction and $a_{uv\gamma}$ parametrizes the strength of the interaction between the electric and magnetic order parameters. In the HTI phase, the magnetic order is described by only one irreducible representation, Γ_3, and due to the high symmetry of the Mn moments, it is possible to define σ_u such that under inversion $\sigma_u(k) \rightarrow \sigma_u(k)^*$. The trilinear coupling thus consists only of terms such as $V = \Sigma_\gamma a_\gamma |\sigma_3(k)|^2 P_\gamma$. Since interactions in a Landau expansion must have the symmetry of the paramagnetic phase, this interaction must be invariant under inversion. This requires that a_γ vanishes, so that $P_\gamma = 0$ in the HTI phase. The conclusion remains valid for Tb order with no restriction on the phase between its two orbits.

For the LTI phase, which is described by Γ_2 and Γ_3, there are, however, additional terms such as $V = \Sigma_\gamma b_\gamma \sigma_2(k) \sigma_3(-k) P_\gamma$ + c.c., where c.c. denotes the complex conjugate. For V to be an invariant, P_γ must transform as the product of Γ_2 and Γ_3. That is, the electric polarization must be even under 1 and m_{yz}, and odd under 2_y and m_{xy}. This condition can only be satisfied for an electric polarization along the c axis. Previous dielectric experiments have shown that the electric polarization that develops below the transition to the LTI phase is indeed oriented along the c axis.

The coupling of the magnetic order parameter to electric polarization in $TbMnO_3$ [5] is similar to that in $Ni_3V_2O_8$, which adopts two different incommensurate magnetic structures [14], one of them ferroelectric and described by two irreducible representations. The correct prediction of the electric polarization for both $TbMnO_3$ and $Ni_3V_2O_8$ (Ref. [11]) suggests that magnetoelectricity resulting from a trilinear magnetoelectric coupling term may be commonplace in insulating transition metal oxides with noncollinear incommensurate structures. Accordingly we find less compelling the suggestion [5] that the appearance of ferroelectricity is associated with an incommensurate to commensurate phase transition. Indeed, there is no evidence of a lock-in transition [see Fig. 2(b)] and it therefore appears to be irrelevant from the point of view of ferroelectricity whether the modulated magnetic order is commensurate or truly incommensurate.

In summary, we have determined the magnetic structure of the paraelectric and ferroelectric phases of $TbMnO_3$. We have shown that the paraelectric, magnetically incommensurate phase has sinusoidally modulated collinear magnetic order that does not break inversion symmetry. The ferroelectric phase, however, has noncollinear incommensurate magnetic order described by two irreducible representations, which explicitly breaks inversion symmetry and thus gives rise to electric polarization. The qualitative aspects of magnetoelectric effects in $TbMnO_3$ appear to be accounted for by a trilinear coupling term in a Landau free energy expansion as proposed by Harris *et al.* [10,11]. Understanding the magnitude of the effect will require experimental as well as theoretical work to track lattice, charge, and orbital degrees of freedom through axial-nonaxial parity breaking phase transition in insulators such as $TbMnO_3$. Apart from the fundamental challenge, improved understanding of magnetoelectricity in these systems may help to produce materials for room-temperature applications.

We thank A. Aharony, O. Entin-Wohlman, and A. Ramirez for helpful discussions. This work was supported by the Swiss National Science Foundation under Contract No. PP002-102831. Work at Johns Hopkins University was supported by the DoE through DE-FG02-02ER45983. Work at University of Pennsylvania and Johns Hopkins University was supported in part by the U.S.-Israel Binational Science Foundation under Grant No. 2000073. Work at Rutgers University was supported by the NSF-DMR-MRSEC-05-20471. This work is based on experiments performed at the Swiss spallation neutron source SINQ, Paul Scherrer Institute, Villigen, Switzerland. The work at SPINS is based upon activities supported by the National Science Foundation under Agreement No. DMR-9986442.

[1] G. A. Smolenskii *et al.*, Sov. Phys. Usp. **25**, 475 (1982).
[2] H. Schmid, Ferroelectrics **62**, 317 (1994).
[3] R. E. Cohen, Nature (London) **358**, 136 (1992).
[4] M. Atanasov *et al.*, J. Phys. Chem. A **105**, 5450 (2001).
[5] T. Kimura *et al.*, Nature (London) **426**, 55 (2003).
[6] T. Lottermoser *et al.*, Nature (London) **430**, 541 (2004).
[7] N. Hur *et al.*, Nature (London) **429**, 392 (2004).
[8] S. Kobayashi *et al.*, J. Phys. Soc. Jpn. **73**, 1593 (2004).
[9] D. V. Efremov *et al.*, Nat. Mater. **3**, 853 (2004).
[10] A. B. Harris *et al.* (to be published).
[11] G. Lawes *et al.*, Phys. Rev. Lett. **95**, 087205 (2005).
[12] S. Quezel *et al.*, Physica (Amsterdam) **86B–88B**, 916 (1977).
[13] R. Kajimoto *et al.*, Phys. Rev. B **70**, 012401 (2004).
[14] G. Lawes *et al.*, Phys. Rev. Lett. **93**, 247201 (2004).